Algerian Journal of Research and Technology
https://doi.org/10.58681/ajrt.24080102
A.J.R.T Volume 8 (N°1) (2024) 9 - 17

Realization of an Inexpensive Embedded Pyranometer for measuring the amount of direct incident solar radiation in the visible and near-infrared

H. Naim [1,*], N. Benabadji [1], A. Bouadi [1], H. Abdelatif

[1]*Laboratory for Analysis and Applications of Radiation (LAAR), Department of Physics, University of Science and Technology of Oran (USTO), B.P. 1505 El M'nouar, 31024, ORAN, ALGERIA*
[2]*Institute of Maintenance and Industrial Security, Université d'Oran 2 Mohamed Ben Ahmed, Bir El Djir 48000, Algeria*

***Corresponding author:** houcine.naim@univ-usto.dz

Received. January 03, 2023. Accepted. March 24, 2024. Published Published May 15, 2024.

DOI: https://doi.org/10.58681/ajrt.24080102

Abstract. This paper presents a detailed description of a mini pyranometer (8-bit 2-input). This device is dedicated to measuring direct incident solar radiation, In the visible and near-infrared (using two broad-spectrum photodiodes, BPW21 and BPW34, respectively). This device is often coupled with an automatic recorder (a datalogger) to establish a record of measurements over a long period, to proceed to a good dimensioning of a system of photovoltaic panels on a region in the process of electrification in solar energy. This assembly's realization was centered on using the smallest 8-bit microcontroller existing on the current market, a PIC10F222 of 6 pins only, from the baseline range of the Microchip. This microcontroller is responsible for ensuring all functions available in this device (measurements, controls, and L.U.T schedule management for each sensor concerned), using specialized integrated modules such as a 2-channel 8-bit analog-to-digital converter. Its low consumption (170 amps under 2V, 4MHz) makes it particularly recommended for designing and producing devices with high energy independence.

Keywords. Pyranometer, Solar radiation, 8-bit microcontroller, visible, near-infrared.

INTRODUCTION

Solar radiation is the amount of energy ($W.m^{-2}$) received per unit area when solar radiation reaches Earth's surface through the atmosphere (Kim, 2018; Bouhlala et al., 200; Yacef et al., 2014 ; Bouchouicha et al., 2019 ; Naim et al., 2020). Solar radiation is divided into (Prieto et al., 2009) global solar radiation, UV ray, and IR ray. the global solar radiation, which is the amount of combined energy contained in the direct and diffuse components, is observed by using a pyranometer (Kim, 2018; Roy et al., 2021; Basaran, 2019).

The pyranometer for observing the solar radiation reaching the surface of the earth is manufactured by various companies around the world at a very high cost.

In this paper, we describe in detail the design and implementation of a low-cost device (mini pyranometer), compact and with low power consumption, dedicated to automatically measuring two critical physical parameters: the amount of direct incident solar radiation in the visible and near infrared (Roy et al., 2021; Tiba et al., 2005). These measurements are acquired periodically (one measurement every three seconds) and immediately displayed on a 4-digit 7-segment display (Cameron, 2019), successively displaying the direct incident solar radiation in the visible and near infrared. To minimize this device's current consumption, each measurement's display is kept visible for 1 second (pulsed current, consumed around 8 mA, by each LED diode of the display, one at a time). The mounting is put into standby (sleep mode) for 2 seconds, where the current consumed is reduced to a value below 1µA. The unit is powered by a 4.5V flat battery or three 1.5V LR6 batteries connected in series. Knowing that its capacity ranges from 500 mA (carbon-zinc type), 1000 mA (alkaline type) to 3000 mA (lithium type), this device's continuous operation time is 62 hours, 125 hours, or 375 hours. Since it is a device for intermittent use, if we assume a daily reading of measurements of less than an hour, its autonomy can be significant (several months).

Fig.1. Overview of the realized device.

DESCRIPTION OF HARDWARE

The synoptic diagram of this assembly comprises the following main modules:

• an 8-bit microcontroller (PIC10F222),

• a 4-digit 7-segment display module,

• an input stage with two measurement channels (direct incident visible radiation, direct incident near-infrared radiation) with a single bipolar transistor preamplifier.

The regulated power supply has a precise voltage of +2.56V, which is well suited to the analog-to-digital converter. With this accurate value, we have a resolution of 10 mV per digital count.

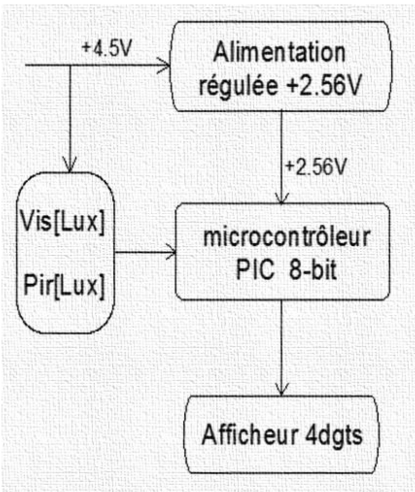

Fig. 2. Block diagram of the device produced.

The 8-bit microcontroller (PIC10F222)

This 8-bit microcontroller has only 6 pins, and because of this, it is considered the smallest microcontroller in the current market. It is part of the baseline range of the American company Microchip (Roy et al., 2021; Arbuzov, 2021; Khadidja et al., 2015 ; Houcine et al., 2015), which has become the world leader in this category of programmable digital components. It has a RISC architecture (with only 33 instructions), whose performance in terms of execution speed and memory occupation rate are much better than the old CISC architecture (for example, Motorola 68705 or Intel 8051). It is powered by a DC voltage ranging from 2.0V to 5.5 [V]; in our case, we used a flat 4.5V battery.

Regarding the operating requirements of the internal 8-bit resolution ADC analog-to-digital conversion module, a precise voltage of 2.56 V was used as a regulated power supply. Indeed, with an 8-bit resolution, we have 256 measurement steps, and by setting the reference voltage to 2.56 V, we obtain a sensitivity of 2560 / 256 = 10 mV.

Finally, this microcontroller has an internal oscillator of 4 and 8 MHz, with a precision of 1%. Two factors were essential in our assembly: the accuracy of the measurements (hence the need for a regulated power supply) and the energy autonomy.

For this last point, we have chosen to drive the 4-digit display in dual multiplexing mode with a single LED lit during the activation of a digit, resulting in a pulsed current of 8 mA, with very low flickering due to multiplexing for 1 second, then to space out the measurements with a dead time of 2 seconds, where the microcontroller is put in standby mode. Thus consuming a current of less than 1 µA.

Finally, the quiet time of 2 seconds between successive measurements and managed by the internal module called WATCHDOG, this module and used to reactivate the PIC (which was put on standby) after 2 seconds to proceed to the subsequent measurement (then it is put back on the back burner, and so on…).

The 4-digit 7-segment led display module

The classic 7-segment LED 4-digit display module requires 12 lines (inputs/outputs) from the PIC (Cameron, 2019), as shown in the following diagram:

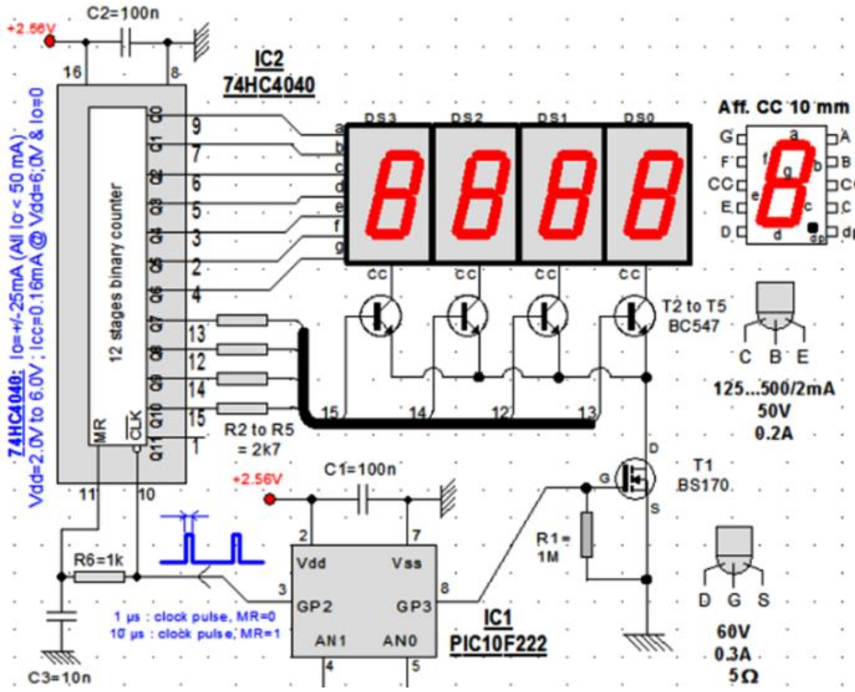

Fig. 3. 4-digit 7-segment LED display module with a 12-bit binary counter.

The PIC10F222 has only 6 pins; We encountered this demo with a 12-bit binary counter, 74HC4040, using the following method: To display, for example, a digital count of 195, the PIC sends a burst of 195 pulses very quickly (each pulse lasts 1 µs), while the MOSFET transistor T1, a BS170, is held off to turn off the display. Then T1 is made conductive for 1 second to read the value of this digital count. Finally, the PIC sends a longer final pulse of 10 µs to reset the binary counter 74HC4040, and the MOSFET transistor T1 is again kept blocked to turn off the display to reduce the consumption of this assembly. The RC cell (resistor R6 and capacitor C3) was designed to drive the two MR and CLK inputs of the 74HC4040 binary counter by a single output of the PIC.

The two analog inputs of the PIC10F222 have been dedicated to measuring the two crucial physical parameters for a pyranometer: the direct incident radiation of the visible (in Lux) and the direct incident radiation of the near-infrared (in Lux). For the visual radiation measurement, a photodiode type BPW21 (Pai and Santra, 2021; Hernandez, 2008; Jian et al., 2016) was preferred, given its broad spectrum of sensitivity, centered on 550 nm. To measure near-infrared radiation, we used a BPW34-type photodiode (Bayhan, 2006; Ozden, 2007), whose sensitivity spectrum is centered on 950 nm. One of the two measurement inputs is preceded by a preamplifier with a single PNP transistor. A maximum measurement of 2.56 V can be read at 2.56 mA across an accurate 1 kilo-Ohm resistor. Using a transistor with a beta gain of only 100 would result in a reading of 25.6 µA. Reading the datasheet of a BPW34 offers various interesting graphs, whose graph illuminates [Lux] as a function of the reverse current Ir [µA] crossing this photodiode. A table has been programmed in the PIC to have a final reading in Lux.

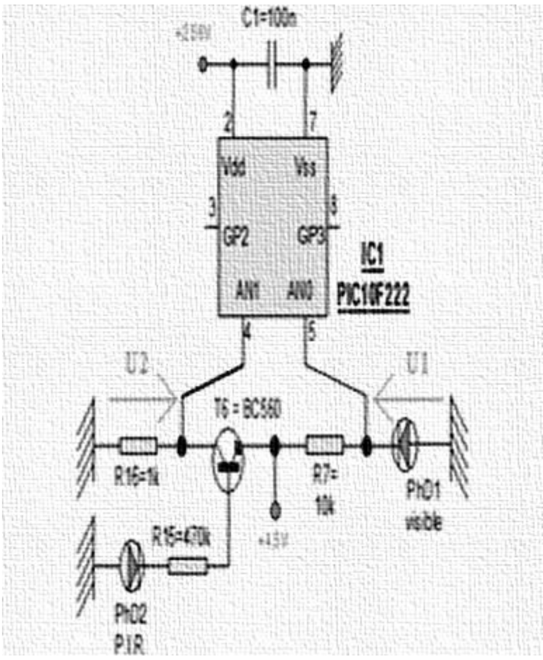

Fig. 4. Input stage for 2 analog measurement channels.

Regulated power supply 2.56V

The regulated power supply section produces a precise voltage of 2.56V from one 4.5V coin cell battery or three 1.5V R6 batteries in series. The choice of the value of 2.56 V was dictated to obtain a measurement step of 10 mV for coding 8 bits (256 possible measurements). The actual current consumed by this power supply is of the order of 150 µA only (Stallon et al., 2012). The transistor (Ta) makes it possible to minimize the fluctuations of the output voltage due to the different variations of the output current and maintains this output voltage at 2.56 V, thanks to the diode (Da), which offers a reference voltage of 0.6 V The ballast transistor (Tb) makes it possible to supplement an output current of up to the order of 100 mA without noticeable heating.

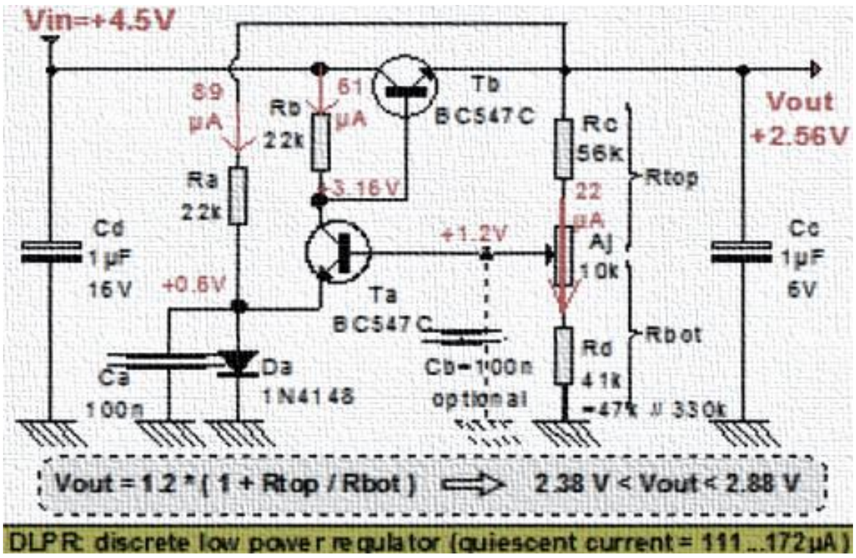

Fig. 5. Discrete regulated power supply, with very low self-consumption.

FIRMWARE DESCRIPTION

The 8-bit microcontroller (PIC10F222) was programmed in assembler with MPLAB v7.52 (Jayaraman and Bin Basiron, 2013), following a modular logic: the main file and associated secondary files.

The 1st file (PYRANO.ASM) contains the main program responsible for configuring the internal modules that will be used later:

- The WATCHDOG module is designed to wake up the PIC from SLEEP mode after 2 s.
- The 8-bit ADC converter and its two inputs, AN0 and AN1

The main program momentarily displays the value 8888 to assure the user of the excellent condition of each segment of the four digits of the display, then proceeds to the 1st measurement and displays it for 1 second, then enters standby mode, thanks to the SLEEP instruction (for minimum current consumption). It will be woken up after (2)s by the WATCHDOG circuit. To proceed to the subsequent measurement, display it, then enter SLEEP mode again. This module is activated only during the measurement phase of a physical parameter, then immediately deactivated To minimize the current consumption of the PIC. Finally, the second file (16B3DGT.INC) is used to convert any 8-bit binary value into a 3-digit decimal value, necessary beforehand before any display.

RESULTS AND DISCUSSION

The measurement results (visible and near-infrared in LUX) can be viewed alternately on display, as shown in Figures 6 and 7.

Fig.6. Display of direct incident visible radiation measurement.

Fig.7 .Display of near-infrared incident radiation measurement.

As shown in figure 8, a system block diagram for a mini pyranometer (8-bit 2-input) has been developed.

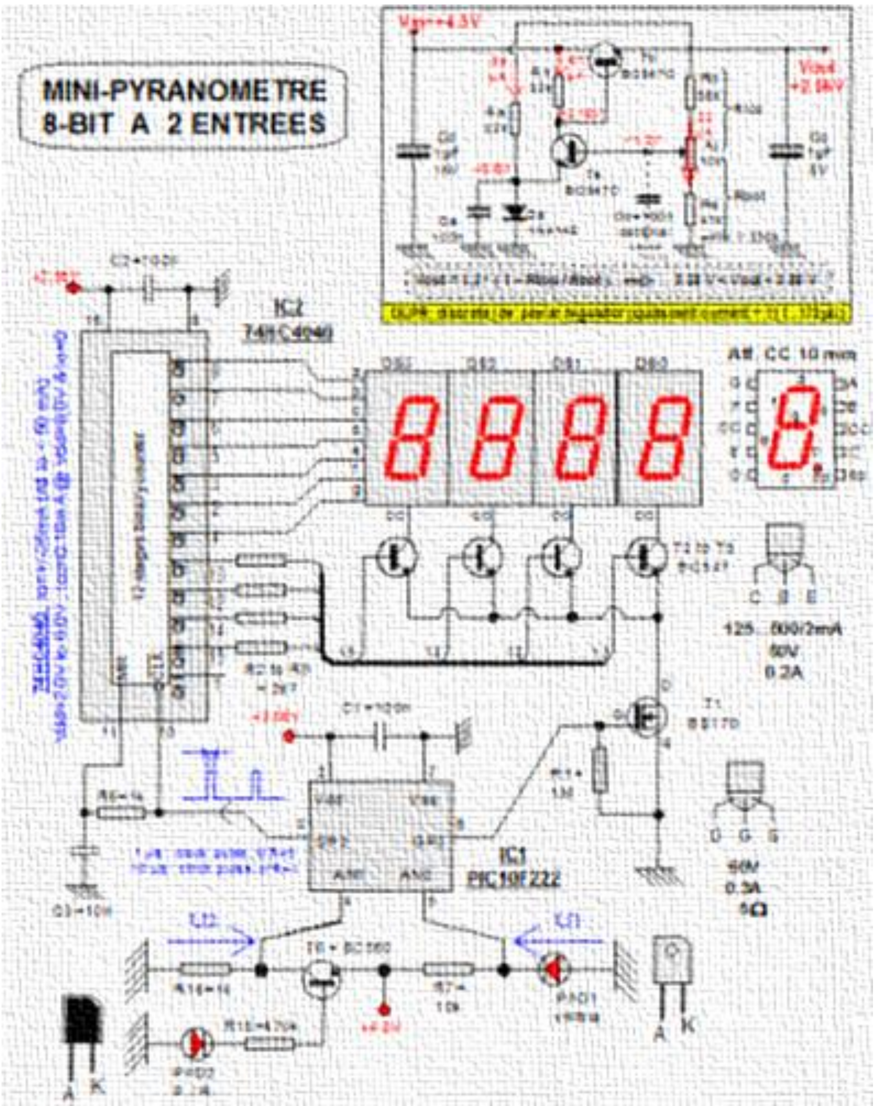

Fig.8. Detailed and complete diagram of the device produced.

CONCLUSION

The most trustful sensor to use is a pyranometer, often based on a thermopile. They are expensive, and for this reason, in this work, we presented the developed circuit innovative, a low-cost sensor for measuring two critical physical parameters: the amount of direct incident solar radiation in the visible and near-infrared.

The cost of manufacturing the device can be estimated as follows. The cost of components, manufacturing a printed circuit board, assembly, housing, and software firmware is almost the same. In total, $27 (at today's prices) is a meager price compared to the devices currently on the market.

REFERENCES

Kim, B. Y., Lee, K. T., Zo, I. S., Lee, S. H., Jung, H. S., Rim, S. H., & Jang, J. P. (2018). Calibration of the pyranometer sensitivity using the integrating sphere. *Asia-Pacific Journal of Atmospheric Sciences*, *54*, 639-648.

Bouhlala, M. A., Naim, H., & Larabi, M. E. A. (2020, March). Estimating Solar Irradiance at the Earth's Surface Using Remote Sensing: Case of Algerian Oranie's Region. In *2020 Mediterranean and Middle-East Geoscience and Remote Sensing Symposium (M2GARSS)* (pp. 261-264). IEEE.

Yacef, R., Mellit, A., Belaid, S., & Şen, Z. (2014). New combined models for estimating daily global solar radiation from measured air temperature in semi-arid climates: application in Ghardaïa, Algeria. *Energy conversion and management*, *79*, 606-615.

Bouchouicha, K., Hassan, M. A., Bailek, N., & Aoun, N. (2019). Estimating the global solar irradiation and optimizing the error estimates under Algerian desert climate. *Renewable energy*, *139*, 844-858.

Naim, H., Fares, R., Bouadi, A., Hassini, A., & Noureddine, B. (2020). An improved model of estimation global solar irradiation from in situ data: case of algerian oranie's region. *Journal of Solar Energy Engineering*, *142*(3), 034501.

Prieto, J. I., Martínez-García, J. C., & García, D. (2009). Correlation between global solar irradiation and air temperature in Asturias, Spain. *Solar Energy*, *83*(7), 1076-1085.

Roy, S., Panja, S. C., & Patra, S. N. (2021). An embedded system to measure ground-based solar irradiance signal. *Measurement*, *173*, 108598.

Basaran, K. (2019). Effect of irradiance measurement sensors on the performance ratio of photovoltaic power plant under real operating conditions: an experimental assessment in Turkey. *Journal of Electrical Engineering & Technology*, *14*(6), 2607-2618.

Tiba, C., De Aguiar, R., & Fraidenraich, N. (2005). Analysis of a new relationship between monthly global irradiation and sunshine hours from a database of Brazil. *Renewable Energy*, *30*(6), 957-966.

Khadidja, B., Amine, B. S., & Noureddine, B. (2015). Prototyping a Dedicated Photovoltaic System Datalogger. *TELKOMNIKA Indonesian Journal of Electrical Engineering*, *16*(3), 488-494.

Houcine, N., Abdelatif, H., Noureddine, B., Fatima Zohra, F., & Abed, B. (2015). Realization of an Inexpensive Embedded Mini-Datalogger for Measuring and Controlling Photovoltaic System. *Journal of Solar Energy Engineering*, *137*(2), 024502.

Pai, H., & Santra, R. (2021). Detection of β+ particle with the low-cost BPW21 Si photodiode. *Nuclear Instruments and Methods in Physics Research Section A: Accelerators, Spectrometers, Detectors and Associated Equipment*, *1005*, 165382.

Hernandez, W. (2008). Linear robust photometer circuit. *Sensors and Actuators A: Physical*, *141*(2), 447-453.

Oyelami, S., Azeez, N. A., Ologunye, O. B., Adeyi, A. J., Adegboye, T. A., Olawale, O. K., & Olawuyi, O. A. (2021). Development of a low-cost wireless data logging Pyranometer with inbuilt temperature and humidity monitoring system. *Environmental Challenges*, *5*, 100219.

Deng, J. Z., Yao, M., Cheng, X. H., & Deng, Z. H. (2016). A real-time VLC to UART protocol conversion system. *Optoelectronics Letters*, *12*(4), 299-303.

Bayhan, H., & Özden, Ş. (2006). Forward and reverse current–voltage–temperature characteristics of a typical BPW34 photodiode. *Solid-state electronics*, *50*(9-10), 1563-1566.

Bayhan, H., & Özden, Ş. (2007). Frequency dependence of junction capacitance of BPW34 and BPW41 pin photodiodes. *Pramana*, *68*, 701-706.

Stallon, S. D., Kumar, K. V., & Kumar, S. S. (2012). High efficient module of boost converter in PV module. *International Journal of Electrical and Computer Engineering (IJECE)*, *2*(6), 758-781.

Jayaraman, R., Basiron, H. B., & Sanga Pillai, P. M. (2013). Programming Microcontroller via Hierarchical Finite State Machine. In *Intelligent Robotics Systems: Inspiring the NEXT: 16th FIRA RoboWorld Congress, FIRA 2013, Kuala Lumpur, Malaysia, August 24-29, 2013. Proceedings 16* (pp. 454-463). Springer Berlin Heidelberg.